
MEASUREMENT OF DUST GRAIN CHARGE IN A WEAKLY IONIZED PLASMA OF A DC DISCHARGE

S. KHRAPAK, S. RATYNSKAIA, A. ZOBININ¹, M.H. THOMA,
M. KRETSCHMER, A. USACHEV¹, V. YAROSHENKO,
R.A. QUINN, G.E. MORFILL, O. PETROV¹, V. FORTOV¹

UDC 533.9
© 2005

Centre for Interdisciplinary Plasma Science,
Max-Planck-Institut für extraterrestrische Physik
(Garching D-85741, Germany),

¹Institute for High Energy Densities, Russian Acad. Sci.
(13/19, Izhorskaya Str., Moscow 125412, Russia)

The charge of dust particles is determined experimentally in a bulk dc discharge plasma in the pressure range 20 – 150 Pa. The charge is obtained by two independent methods: One is based on an analysis of the particle motion in a stable particle flow and another on an analysis of the transition of the flow to an unstable regime. Molecular dynamics simulations of the particle charging under conditions similar to those of the experiment are also performed. The results of both experimental methods and the simulations demonstrate good agreement. The charge obtained is several times smaller than predicted by the collisionless orbital motion theory, and thus the results serve as an experimental indication that ion-neutral collisions significantly affect the particle charging.

Introduction

Dusty (complex) plasmas constitute ionized gases containing charged particles (grains) of condensed matter. Dust and dusty plasmas are quite natural in space: they are present in planetary rings, comet tails, and interplanetary and interstellar clouds [1–3]. Dust particles are often present in plasmas used for industrial applications [4, 5] and in thermonuclear facilities with magnetic confinement [6, 7]. It is also recognized that, under laboratory conditions, complex plasmas can exhibit properties of crystals, liquids, and gases depending on the strength of the interaction between grains. In addition, the overall dynamical time scales associated with the grain component are relatively long, and grains can be easily visualized. The unique feature of observing the kinetic properties in real space and time provides the opportunity to study the generic universal processes (e.g., phase transitions, crystallization, transport and wave phenomena, self-organization and scaling in fluid flows, etc.) in details not possible so far, and at a more fundamental level [8–12]. Not surprisingly, the field of dusty plasmas has received

considerable attention and has been growing constantly over last decades.

The grain charge is one of the most important parameters of dusty plasmas. In typical laboratory experiments using gas discharges the (negative) charge on a grain is determined by the balance of electron and ion fluxes to its surface. To calculate these fluxes the orbital motion limited (OML) theory (see, for example, [13, 14]) is usually used. This approach deals with collisionless electron and ion trajectories in the vicinity of a small individual probe (dust grain) and allows the determination of the cross sections for electron and ion collections only from the laws of conservation of energy and angular momentum. However, the assumptions underlying OML theory are seldom met in real dusty plasmas. Let us discuss three major reasons which can make the OML approach inapplicable.

The first is associated with a finite dust density in experiments and is known as the effect of “closely packed” grains. This effect is two-fold. The grain component contributes to the quasineutral condition, making the ion density larger than the electron density [15]. This increases the ratio of the ion-to-electron current and hence reduces the absolute value of the grain charge as compared to that in the case of an individual grain. The strength of the effect can be characterized by the parameter $P = Z_d n_d / n_e$ (often called the Havnes parameter), where Z_d is the absolute magnitude of grain charge in units of elementary charge and n_d (n_e) is the grain (electron) number density. The charge tends to the charge of an individual grain when $P \ll 1$, whilst it is reduced considerably for $P \gg 1$. In addition, when the intergrain separation Δ is smaller than the plasma screening length λ_D then the ion and electron trajectories are affected by neighboring grains, which can also influence the grain charging. In [16], it was demonstrated experimentally that the effect of

“closely packed” grains can lead to a substantial charge reduction.

The second reason is associated with the fact that the OML theory presumes the absence of a barrier in the *effective* potential energy of interaction between a probe and plasma particles. The barrier is absent for repulsive interaction (i.e., for electrons) but can be present for attractive interaction (i.e., ions). It can be shown that the barrier is absent only when the electrostatic potential around the probe decays more slowly than $1/r^2$ [17]. In reality, however, the potential scales as $\propto 1/r$ closely to the probe, $\propto 1/r^2$ far from it, and the potential can decrease faster at intermediate distances. As a result, the barrier in the effective potential energy emerges for ions moving to the probe: some (low-energy) ions are reflected from this barrier and cannot reach the probe surface. This effect leads to a decrease in the ion current compared to the OML theory and, hence, to an increase in Z_d . For a Maxwellian ion velocity distribution, there are always sufficiently slow ions which are reflected from the barrier in the effective potential energy [18]. However, it can be shown that, for a model screened Coulomb interaction potential, the corrections to OML are small as long as the grain radius is considerably smaller than the screening length [12, 19, 20]. The same conclusion is drawn in [14] from a consistent solution for the surface potential, potential distribution around a probe, and distribution of ion trajectories.

The third reason is due to ion-neutral collisions. In the OML approach collisions of electrons and ions are neglected on the basis that the electron and ion mean free paths $\ell_{e(i)}$ are long compared to the plasma screening length. However, theory has shown that ion-neutral charge exchange collisions in the vicinity of a small probe or a dust grain can lead to a substantial increase in the ion current to their surfaces [21–23]. It has been demonstrated that ion collisions can suppress the grain charge even when ℓ_i is considerably greater than λ_D . In [24, 25], an enhancement of the ion current to a cylindrical Langmuir probe due to charge-exchange collisions was reported.

The examples of applying the simple OML theory to real complex plasmas show the importance of experimental investigation of particle charging. So far most of the experiments were performed in the sheath or striation regions of discharges [26–32]. The comparison with theory is complicated here due to a strong plasma anisotropy and non-neutrality, the presence of “suprathermal” ions and electrons, etc. In addition to the charging model one needs to choose an appropriate model for the sheath, which is itself a sophisticated task.

Hence, there is clearly a lack of direct measurements of the particle charge in bulk plasmas.

In this paper, we present the experimental results on the dust particle charge in a plasma in a wide range of neutral gas pressures. The emphasis of the experiment is on the effect of ion-neutral collisions on grain charging. The experiment is performed with particles of radius $a = 0.6 \mu\text{m}$ in a horizontal dc discharge tube. For these particles the weak ambipolar radial electric field in the bulk plasma is sufficient to compensate gravity allowing us to study the dust charging in a quasineutral plasma. Highly space and time-resolved measurements of the particle flow and comprehensive probe measurements of plasma parameters make it possible to use theoretical models where the only unknown parameter is the particle charge. This enables us to determine the charge experimentally by two independent methods. The results are then compared with those of MD simulations and theory.

1. Experiment

The experiment is performed in a dc discharge generated in an U-shaped glass tube, the PK-4 facility (see sketch in [33]), and operated in neon at pressures 20 – 150 Pa and current of 1 mA (voltage of 1 kV). The plasma parameters at different pressures are measured in the absence of dust grains using a Langmuir probe. The description of the probe measurements and results can be found in [34]. The dependences of the measured axial values of electron density n_e , electron temperature T_e , and electric field E can be well fitted by the following expressions linear in pressure: $n_e = 10^8 \times (0.918 + 0.028p)$ cm^{-3} , $T_e = 8.349 - 0.022p$ eV, and $E = 2.08$ V/cm, where p is the pressure in Pa. The ion temperature is assumed to be close to the neutral gas temperature, $T_i \simeq T_n \simeq 0.03$ eV, for the pressure range used.

When the dust particles (melamine-formaldehyde spheres with a mass density of 1.51 g/cm^3) are injected into the discharge, they are charged negatively and drift against the discharge electric field in the horizontal part of the tube (see Fig. 2 in [33]). The particle flow is illuminated by a laser sheet of a width of $(100 \pm 30) \mu\text{m}$. The particle motion is recorded by a video camera with a field of view of $6.4 \times 4.8 \text{ mm}^2$ and a rate of 120 frames per second. Each image corresponds to an exposure time of 8 ms. From an analysis of the digitized video the dust number density n_d can be estimated by counting the number of particles in single snapshots. The particle velocities, V_d , can be obtained by tracking individual particles through the video sequence.

We study the particle dynamics varying the neutral gas pressure p and the number of injected particles N_d (controlled by settings of a particle dispenser). This allows us to determine the dust particle charge by two different methods. For a sufficiently low number of particles, the flow is stable for all pressures studied. The flow pattern is recorded for a number of different pressures. The charge is then estimated from the force balance condition using the experimentally found particle velocities.

For larger N_d , the transition to unstable flow with a clear wave behavior occurs at a certain threshold pressure p_* [34, 35]. The transition is a manifestation of the ion-dust streaming instability caused by a relative drift between the dust and the ion components. The value of p_* depends on N_d (shifting towards higher pressures when N_d is increased). In this case, the charge is estimated from a linear dispersion relation describing the transition of the particle flow to an unstable regime at p_* . In addition, the force balance condition for pressures just above (1 – 4 Pa) p_* is used to estimate the charge.

2. Theoretical Models

Below we present theoretical basis for the two methods which are used for the charge estimation.

2.1. Force balance

The particle velocity in a stable flow is determined by the balance of the forces acting on particles: the electric force, $F_{el} = -Z_d e E$, neutral drag force, $F_n = -m_d \nu_{dn} V_d$, ion drag force, $F_i = m_d \nu_{di} (u_i - V_d) \simeq m_d \nu_{di} u_i$, and electron drag force $F_e \simeq m_d \nu_{de} u_e$. Here, m_d is the dust particle mass, u_i (u_e) is the ion (electron) drift velocity, ν_{dn} , ν_{di} , and ν_{ed} are the momentum transfer frequencies in dust-neutral, dust-ion, and dust-electron collisions, respectively. Under our conditions, the electron drag force is almost two orders of magnitude smaller than the ion drag force due to the large value of electron-to-ion temperature ratio (see [36] for details). Thus, the force balance is

$$F_{el} + F_i + F_n \simeq 0. \quad (1)$$

For the momentum transfer in dust-ion collisions, we use

$$m_d \nu_{di} = \frac{8\sqrt{2\pi}}{3} a^2 n_i m_i v_{T_i} \left(1 + \frac{1}{2} \frac{R_C}{a} + \frac{1}{4} \frac{R_C^2}{a^2} \Lambda \right), \quad (2)$$

where $R_C = Z_d e^2 / T_i$ is the Coulomb radius for ion-dust collisions, m_i is the ion mass, $v_{T_i} = \sqrt{T_i / m_i}$ is the

ion thermal velocity, and $\Lambda = \int_0^\infty \exp(-x) \ln[(2\lambda_D x + R_C) / (2ax + R_C)] dx$ is the *modified* Coulomb logarithm integrated over the Maxwellian velocity distribution function for ions [37]. In deriving Eq. (2) a subthermal ion drift ($u_i \lesssim v_{T_i}$) is assumed, which means that the effective screening length is close to the ion Debye radius, $\lambda_D \simeq \lambda_{Di} = \sqrt{T_i / 4\pi e^2 n_i}$ [38]. Expression (2) is applicable at a moderate coupling between a grain and ions, $R_C / \lambda_D \lesssim 5$ [37, 39, 40], which is the case for the relatively small grains and plasma conditions investigated. In addition, it is derived for collisionless ions, $\ell_i \gg \lambda_D$. Although, this is not the case in our experiments, our estimates based on the model developed for the ion drag force in *collisional* plasma in the regime of weak ion-grain coupling [41] show that the contribution of ion-neutral collisions to the ion drag is small at $p \lesssim 100$ Pa. At higher pressures the ion drag force is a small fraction of the electric force acting on grains, and some inaccuracy caused by neglecting collisions does not have considerable effect on the charge estimation.

From the momentum conservation, we have $\nu_{id} = \nu_{di} (m_d n_d / m_i n_i)$, where ν_{id} is the momentum loss frequency of the ions in ion-dust collisions. For the momentum transfer in dust-neutral collisions, we have $m_d \nu_{dn} = (8\sqrt{2\pi}/3) \delta a^2 n_n m_n v_{T_n}$, where m_n , n_n , and v_{T_n} are the mass, density, and thermal velocity of neutrals, respectively [42]. The numerical factor $\delta = 1 + \pi/8 \simeq 1.4$, corresponding to diffuse scattering with full accommodation is chosen in accordance with recent experimental results [43]. The ion drift velocity is determined by ion-neutral and ion-dust collisions, $u_i \simeq eE / m_i \nu_i^{\text{eff}}$, where $\nu_i^{\text{eff}} = \nu_{in} + \nu_{id}$. The frequency ν_{id} is given above. For ν_{in} , we use an estimate $\nu_{in} = n_n \sigma_{in} v_{T_i}$, with the effective momentum transfer cross section taking into account both the charge exchange and polarization interactions, $\sigma_{in} \simeq 10^{-14} \text{ cm}^2$ [44, 45].

2.2. Linear dispersion relation

Though a linear theory might not be applicable to describe the wave mode observed in the experiment (e.g., wavenumber and frequency), it should be adequate to predict the onset of self-excited waves at p_* . In the derivation of a dispersion relation, the following effects are taken into account: electron, ion, and dust collisions with neutrals, ion-dust collisions, and drifts of the electron, ion, and dust components relative to the stationary neutral gas. We also assume “warm” electrons

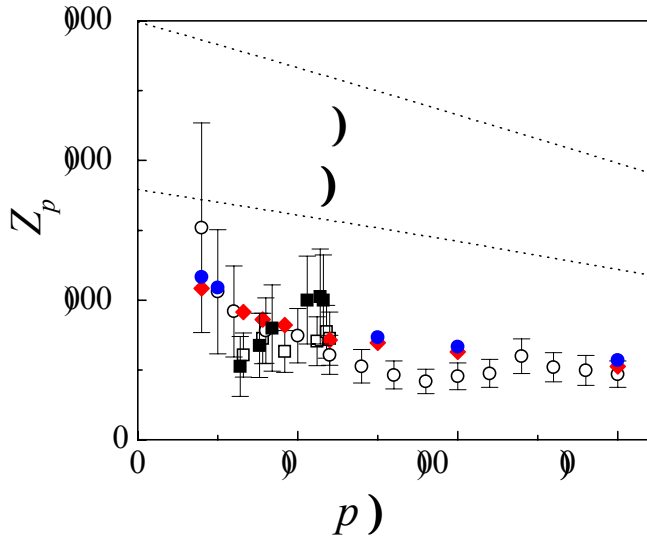


Fig. 1. Grain charge obtained from experiments [force balance for a low number of injected particles (open circles); force balance for pressures above the threshold (open squares), solution of the dispersion relation (solid squares)] and from MD simulations (diamonds for finite grain density and solid circles for an individual grain). The area between two dotted lines corresponds to the charge given by the OML model for the Havnes parameter between $P = 0.2$ (upper line) and $P = 3$ (lower line)

and ions and “cold” dust. Using the hydrodynamic approach, we get

$$1 + \chi_e + \chi_i + \chi_d = 0, \quad (3)$$

where

$$\chi_\alpha = \frac{\omega_{p\alpha}^2}{k^2 v_{T\alpha}^2 \mp k u_\alpha (i \nu_{\alpha n} \pm k u_\alpha)}$$

are the susceptibilities of the electron ($\alpha = e$) and ion ($\alpha = i$) components (the upper sign in the denominator is for electrons), and

$$\chi_d = -\frac{\omega_{pd}^2}{(\omega + kV_d)(\omega + kV_d + i\nu_{dn})}$$

is the susceptibility of the dust component. Here, k and ω are the wavenumber and frequency, $\omega_{pi(e)} = v_{T_{i(e)}}/\lambda_{Di(e)}$ is the ion (electron) plasma frequency, and $\omega_{pd} = \sqrt{4\pi Z_d^2 e^2 n_d/m_d}$ is the dust plasma frequency. Compared to the dispersion relation derived in [35], expression (3) takes into account the electron drift. Note also that there is a misprint in [34] in the dust grain susceptibility (χ_d), where ω appeared instead of $\omega + kV_d$. The electron-neutral collision frequency and electron

drift velocity are given by $\nu_{en} = n_n \sigma_{en} v_{Te}$ and $u_e = eE/m_e \nu_{en}$, respectively. In a neon plasma with $T_e \gtrsim 1$ eV, the momentum transfer cross section for electron-neutral collisions is almost constant, $\sigma_{en} \simeq 2 \times 10^{-16}$ cm² [46].

3. Results and Discussion

We solve Eqs. (1) and (3) numerically for the plasma parameters taken from probe measurements. The ion density is obtained from the quasineutrality condition $n_i = n_e + Z_d n_d$. We assume that n_e is unaffected by the presence of dust, but n_i is increased. This assumption is supported by our estimates showing that, for the grain component uniformly filling the discharge tube, the electron mobility is unaffected by dust, and the electron loss to particles is smaller than that due to the recombination on walls at densities below $n_d \sim 5 \times 10^5$ cm⁻³. The latter means that, for smaller densities, the ionization/recombination balance of electrons is not changed by the presence of grains and neither are T_e and E . For the dc discharge at a constant current, $I \propto n_e E$, we conclude that the average value of n_e is also unaffected by dust. We found experimentally that $p_* \sim 60$ Pa at $n_d \sim 5 \times 10^5$ cm⁻³ for the transition to an unstable regime. Thus, the applicability of the linear dispersion relation method is limited to pressures below 60 Pa.

With the assumption made, the parameters n_i , ν_{di} , ν_{id} , u_i , ω_{pi} , and ω_{pd} are functions of the particle charge only. Equation (1) is solved directly, yielding the particle charge. Solving the dispersion relation (3) gives the dependence of $\omega = \omega_r + i\omega_i$ on the wavenumber k for a given particle charge. The charge is then determined by matching the experimental observations: stable mode ($\omega_i < 0$ for all k) above the threshold pressure p_* and unstable mode ($\omega_i > 0$ for a range of k , corresponding to experimentally found wavelengths) below p_* . More details on the solving procedure and illustrations can be found in [34, 35]. The results of both methods are presented in Fig. 1 and demonstrate good agreement. The error bars correspond to the uncertainties in n_d (50%), n_e (30%), E (10%), and V_d (15%). Both methods are quite insensitive to the value of T_e .

To have an independent verification of the charge estimates described above, MD simulations of particle charging have been carried out for conditions similar to those of the experiment. The simulations are performed using a code originally developed in [21] to study the effect of ion-neutral collisions on the charge of an individual particle in a quasineutral plasma. [Some

modifications are made to the code to take into account a finite n_d . We omit the details of the modifications, because the difference between the charges obtained using the original and the modified codes is not significant for our conditions (see Fig. 1).] As seen from Fig. 1, the charges found from the simulations are in good agreement with the results of both experimental methods.

Figure 1 shows the results of theoretical charge calculations for the range of the Havnes parameter, $0.2 \lesssim P \lesssim 3$, estimated from experimentally determined charges. We use the OML expression modified to take into account the contribution of dust to the quasineutrality condition, $v_{T_e} \exp(-Z_d e^2/aT_e) = v_{T_i} (1 + Z_d e^2/aT_i)(1 + P)$ [12]. The difference between the OML theory and the charges found from experiments and MD simulations is most significant at higher pressures. At $p \sim 100$ Pa we have $P \simeq 0.2$, $\Delta/\lambda_D \simeq 3.6$, and $\ell_i/\lambda_D \simeq 0.6$. This means that the quasineutrality is weakly affected by dust ($P \ll 1$), and so are electron and ion trajectories by surrounding grains ($\Delta \gg \lambda_D$). Thus, the effect of “closely packed” grains is insignificant in this regime. Therefore, we attribute the dramatic charge suppression (up to 5 times) at higher pressures to the effect of ion-neutral collisions. For the lowest pressures investigated, $\ell_i/\lambda_D \sim 3$ and the charge tends towards the OML values, as expected from theory [14, 21]. Some difference still exists and can be caused by a combination of all the effects mentioned above.

In Fig. 2, we plot the normalized grain charge $z = Z_d e^2/aT_e$ as a function of the “collisionality” parameter λ_D/ℓ_i . The charge decreases with increase in the collisionality, as expected from theory [21, 23]. The values of z are in the range from ~ 1 to ~ 0.3 , which does not contradict the values of $z \sim 0.4$ (at $p \simeq 25$ Pa) [47] and $z \sim 0.8$ (at $p \simeq 12$ Pa) [48] found in recent experiments under microgravity conditions using the excitation of low-frequency waves in the grain cloud. A more detailed comparison is useless because the experiments were performed under completely different plasma conditions (e.g., different types of discharges, different gases, different plasma parameters). At the same time, these numbers suggest that $z \lesssim 1$ for a typical quasineutral dusty plasma instead of the popular assumption that z is “of a few” based on the results of the collisionless OML theory.

Conclusions

In conclusion, we have determined the charge of dust particles in a bulk dc discharge plasma under the

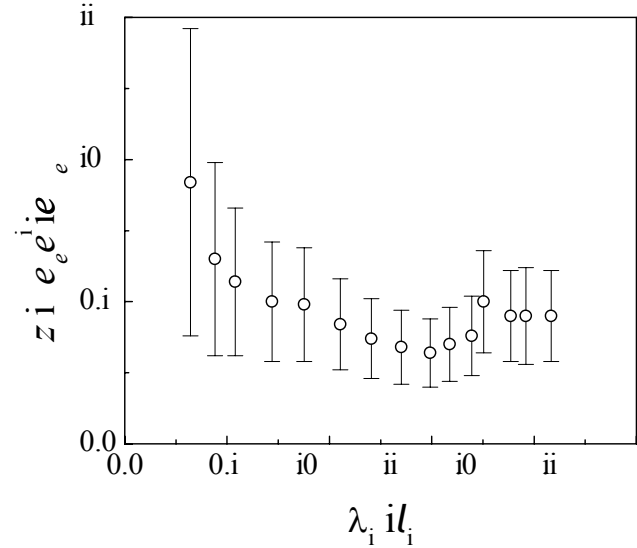


Fig. 2. Grain dimensionless charge $z = Z_d e^2/aT_e$ as a function of the ion “collisionality” parameter, λ_D/ℓ_i . Only the results from the force balance method are shown

conditions when the ion mean free path is comparable to the plasma screening length. Two independent experimental methods and MD simulations agree well with each other and yield a charge which is considerably smaller than that predicted by the collisionless orbital motion theory. Thus, our results prove experimentally the significant effect of ion-neutral collisions on the particle charging in plasmas.

This work was supported by DLR under grant 50 WP 0204.

1. Goertz C.K. // Rev. Geophys. **27** (1989) 271.
2. Bliokh P., Sinitsin V., Yaroshenko V. Dusty and Self-Gravitational Plasmas in Space. — Dordrecht: Kluwer, 1995.
3. Whipple E.C. // Repts. Progr. Phys. **44** (1981) 1197.
4. Boufendi L., Bouchoule A. // Plasma Sources Sci. Technol. **11** (2002) A211.
5. Kersten H. et al. // Contrib. Plasma Phys. **41** (2001) 598.
6. Tsytoovich V.N., Winter J. // Phys. Usp. **41** (1998) 815.
7. Winter J. // Phys. Plasmas **7** (2000) 3862.
8. Thomas H.M., Morfill G.E. // Nature **379** (1996) 806.
9. Morfill G.E. et al. // Phys. scr. **T107** (2004) 59.
10. Morfill G.E. et al. // Contrib. Plasma Phys. **44** (2004) 450.
11. Morfill G.E. et al. // Phys. Rev. Lett. **92** (2004) 175004.
12. Fortov V.E. et al. // Phys. Usp. **47** (2004) 447.
13. Allen J.E. // Phys. scr. **45** (1992) 497.

14. Kennedy R.V., Allen J.E. //J. Plasma Phys. **69** (2003) 485.
15. Havnes O., Morfill G.E., Geortz C.K. //J. Geophys. Res. **89** (1984) 10999.
16. Barkan A., D'Angelo N., Merlino R.L. //Phys. Rev. Lett. **73** (1994) 3093.
17. Al'pert Ya.L., Gurevich A.V., Pitaevskii L.P. Space Physics with Artificial Sattelites. — New York: Plenum Press, 1995.
18. Allen J.E., Annaratone B.M., de Angelis U. //J. Plasma Phys. **63** (2000) 299.
19. Lampe M. //Ibid. **65** (2001) 171.
20. Khrapak S.A., Ivlev A.V., Morfill G. E. //Phys. Rev. E **70** (2004) 056405.
21. Zobnin A.V. et al. //JETP **91** (2000) 483.
22. Lampe M. et al. //Phys. Rev. Lett. **86** (2001) 5278.
23. Lampe M. et al. //Phys. Plasmas **10** (2003) 1500.
24. Sternovsky Z., Robertson S. //Appl. Phys. Lett. **81** (2002) 1961.
25. Sternovsky Z., Robertson S., Lampe M. //J. Appl. Phys. **94** (2003) 1374.
26. Melzer A., Trottenberg A., Piel A. //Phys. Lett. A **191** (1994) 301.
27. Homann A., Melzer A., Piel A. //Phys. Rev. E **59** (1999) R3835.
28. Tomme E.B. et al. //Phys. Rev. Lett. **85** (2000) 2518.
29. Fortov V.E. et al. //Ibid. **87** (2001) 205002.
30. Piel A., Melzer A. //Plasma Phys. Control. Fusion **44** (2002) R1.
31. Samarian A.A., Vladimirov S.V. //Phys. Rev. E **67** (2003) 066404.
32. Ticos C.M., Dyson A., Smith P.W. //Plasma Sources Sci. Technol. **13** (2004) 395.
33. Thoma M.H. et al. //Ukr. Fiz. Zh. This issue, P.179.
34. Ratynskaia S. et al. //Phys. Rev. Lett. **93** (2004) 085001.
35. Ratynskaia S. et al. //IEEE Trans. Plasma Sci. **32** (2004) 613.
36. Khrapak S.A., Morfill G.E. //Phys. Rev. E **69** (2004) 066411.
37. Khrapak S.A. et al. //Ibid. **66** (2002) 046414.
38. Khrapak S.A. et al. //Phys. Plasmas **10** (2003) 4579.
39. Khrapak S.A. et al. //Phys. Rev. Lett. **90** (2003) 225002.
40. Khrapak S.A. et al. //IEEE Trans. on Plasma Sci. **32** (2004) 555.
41. Ivlev A.V. et al. //Phys. Rev. Lett. **92** (2004) 205007.
42. Epstein P.S. //Phys. Rev. **23** (1921) 710.
43. Liu B. et al. //Phys. Plasmas **10** (2003) 9.
44. Biondi M.A., Chanin L.M. //Phys. Rev. **94** (1954) 910.
45. Varney R.N. //Ibid. **88** (1952) 362.
46. Gilardini A. Low Energy Electron Collisions in Gases. — New York: Wiley, 1972.
47. Khrapak S. et al. //Phys. Plasmas **10** (2003) 1.
48. Yaroshenko V.V. et al. //Phys. Rev. E **69**(2004) 066401.

ВИМІРЮВАННЯ ЗАРЯДУ ПОРОШИНОК У СЛАБОІОНІЗОВАНІЙ ПЛАЗМІ ГАЗОВОГО РОЗРЯДУ

*С. Храпак, С. Ратинська, А. Зобнин, М.Х. Тома,
М. Кретчмер, А. Усачьов, В. Ярошенко, Р.А. Куїнн,
Г.Е. Морфілл, О. Петров, В. Фортвов*

Резюме

Двома незалежними методами експериментально визначено заряди порошинок у газорозрядній плазмі при тисках 20—150 Па. Один з методів ґрунтується на аналізі руху частинок у стаціонарному дисперсному потоці, другий — на аналізі переміщення потоку у нестационарному режимі. Виконано моделювання динаміки заряджання частинок для умов експерименту. Результати моделювання узгоджуються з експериментальними даними. Встановлено, що виміряні величини заряду у кілька разів менші ніж ті, що передбачає теорія беззіткнювального орбітального руху. Останнє свідчить про суттєву роль зіткнень іонів з нейтральними частинками.